

Azulene-substituted TTF derivatives†

Hiroshi M. Yamamoto, Jun-Ichi Yamaura and Reizo Kato*

Institute for Solid State Physics, The University of Tokyo, Roppongi Minato-ku, Tokyo 106, Japan

In order to examine Little's model for organic superconductors, several azulene-substituted TTF derivatives were synthesized. Measurements of the oxidation potentials using cyclic voltammetry (CV) provide their donor abilities. The molecular structure of AET (azulenoethylenedithiotetrathiafulvalene) was determined by X-ray analysis. Cation radical salts of synthesized donors with BF_4^- , ClO_4^- , PF_6^- , AsF_6^- and $[\text{Pt}(\text{dmit})_2]^{n-}$ ($\text{dmit} = \text{C}_3\text{S}_5^{2-} = 2\text{-thioxo-1,3-dithiole-4,5-dithiolate}$) were prepared by galvanostatic electrolyses. Temperature-dependent electrical resistances indicate that these salts are all semiconductive. The crystal structure of $(\text{AET})_2[\text{Pt}(\text{dmit})_2]$ was determined by X-ray analysis and its electronic structure is discussed.

Organic molecular conductors have been the subject of considerable interest in physics and chemistry because of their stimulating properties such as their charge density wave,¹ field induced spin density wave,² spin-Peierls transition³ and superconductivity.⁴ In order to reach the superconducting state, a finite value of the density of state should be maintained and thus the metal-insulator transition should be suppressed down to low temperature. Considering that the low-dimensional nature of the system induces a metal-insulator transition, one can understand that an increase of dimensionality of the electronic structure is the current focus in developing molecular superconductors. This strategy has led to the preparation of many molecular conducting materials that exhibit various types of Fermi surfaces.⁵ Some of these materials such as BEDT-TTF [bis(ethylenedithio)tetrathiafulvalene] salts show superconducting behaviour.⁶ It is obvious, however, that the properties of superconductivity, for example the critical temperature (T_c), are governed not only by the geometry of the Fermi surface but also by many other factors.⁷

Little has pointed out that the T_c of organic superconductors can rise to room temperature *via* a special mechanism.⁸ Fig. 1 illustrates his model, a polyacetylene chain substituted by cyanine dye. First, conduction electrons excite the positive charge of the side chains to approach close to the chain backbone. Second, the positive charge attracts another electron and thus provides an attractive force for electrons. Finally, this attractive force brings about the superconductivity. Therefore, an oscillation of positive charge on the side chain takes the place of the phonon in the BCS theory.⁹ In other words, the conventional electron-phonon interaction mechanism is replaced by an electron-exciton mechanism, based on electronic polarization effects.

The high T_c in Little's calculation is achieved because the mass of the electron is much smaller than that of nuclei which can be regarded as an extension of the isotope effect on the T_c of superconductivity. We can, therefore, make use of the electronic polarization component of permeability instead of the ionic part. Electronic polarization has a higher energy than ionic polarization so T_c calculated using Little's theory should be higher than the conventional one.

Little's polymer has not yet been prepared due to synthetic difficulties, although we still consider the theory very attractive. We, therefore, planned to substitute an array of organic radicals for the polyacetylene in order to make his proposal synthetically accessible. To this end, we designed azulene-substituted

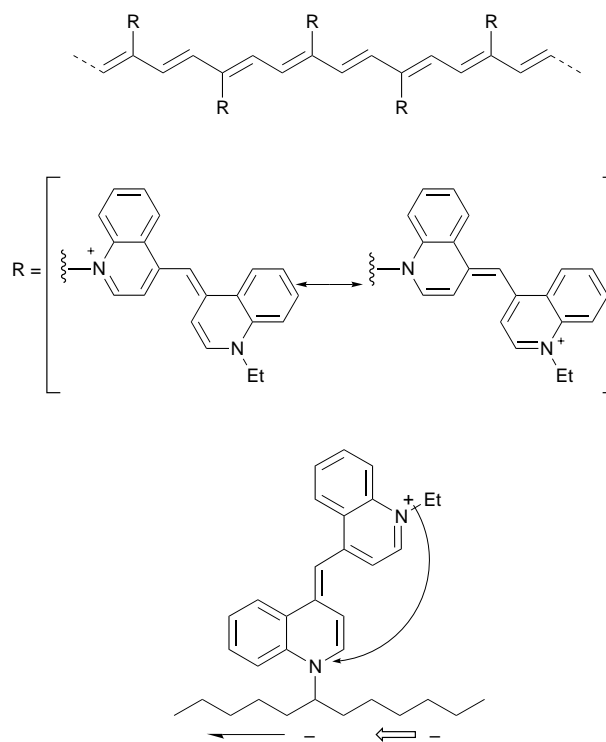


Fig. 1 Illustration of Little's model for high-temperature superconductivity

TTF derivatives. We selected the TTF moiety as a conduction path, and the azulene ring as a source of oscillating dipole.

Our choice of azulene was based on the following. (i) Because azulene consists of five- and seven-membered rings, the 6π aromatic stabilization effect on each ring gives rise to a charge separation in the ground state¹⁰ [Fig. 2(a)]. Azulene therefore has a significant dipole moment with the negative charge on the five-membered ring in the ground state¹¹ (1.08 Debye). In addition, since the coefficients of its LUMO have a tendency to gather on the seven-membered ring [Fig. 2(b)], azulene in the excited state has a dipole moment in the opposite direction¹² (-0.42 Debye). Thus the excitation of an electron on an azulene ring will change the electric environment of the conduction carriers on the TTF moiety. (ii) Excitation of an electron from the HOMO to the LUMO requires little energy (1.8 eV) because the excitation reduces the mutual repulsion between electrons.¹⁰ This small excitation energy enables the conduction carriers on the TTF moiety to utilize the azulene ring as a source of the oscillating dipole.

† Presented at the 58th Okazaki Conference, Recent Development and Future Prospects of Molecular Based Conductors, Okazaki, Japan, 7-9 March 1997.

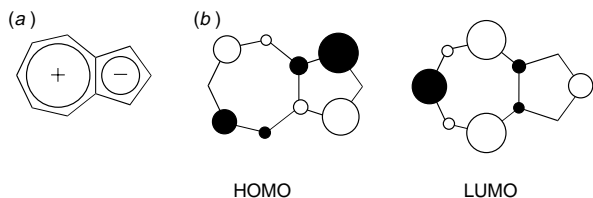


Fig. 2 (a) Charge separation in the azulene ring at its ground state; (b) schematic representation of the coefficients of the azulene HOMO and LUMO

The azulene ring attached to the TTF moiety can thus act as an oscillating dipole. The interaction between conduction carriers on the TTF and the oscillating dipole on the azulene ring should make carriers attractive to each other leading to superconductivity. With this in mind, we have examined azulene-substituted TTF derivatives and this article describes the syntheses, electrochemistry, visible absorption, X-ray analysis and MO calculations of such TTF derivatives as well as the electrical properties and X-ray analysis of their cation radical salts.

Results and Discussion

Synthesis and properties of neutral donors

The synthetic route is presented in Scheme 1. 5,6-Dichloroazulene **1** is converted to trithiocarbonate **3** by the nucleophilic attack of potassium sulfide and subsequent intramolecular ring closure in potassium trithiocarbonate **2**. Azulene-substituted TTF derivatives **5a–5f** were synthesized by the cross-coupling reactions of units **4a–4f** with azulene-containing unit **3** using neat triethyl phosphite. The symmetrical donor, diazulenyl-TTF, was also synthesized by the same method, but it was not characterized in detail because it is a mixture of *cis* and *trans* forms. The yields of coupling reactions were moderate except for the low yield of **5e**. Replacement of the thioketone in the unit **4e** with the ketone did not improve the reaction yield. This low yield was due to the decomposition of the thiadiazole ring.

The electrochemical properties of donors **5a–5f** have been studied by cyclic voltammetry (CV) and the results are listed in Table 1, along with the data for BEDT-TTF as a reference compound. Some of the observed redox peaks were irreversible

donor	E_1/V^a	E_2/V^a	$\Delta E/V = E_2 - E_1$
BEDT TTF	0.12	0.43	0.31
5a	0.17	0.49	0.32
5b	0.15	0.44	0.29
5c	0.16 ^b	0.47 ^b	0.34
5d	0.24 ^b	0.53 ^b	0.29
5e	0.44 ^c	0.84 ^c	0.40
5f	0.24 ^c	0.63 ^c	0.39

^a V_s : Ag/AgNO₃, benzonitrile, 22 °C, Pt working and counter electrodes. ^bQuasi-reversible. ^cIrreversible (E_1 and E_2 values were determined by differential pulse polarography).

probably owing to undesired reaction at the azulene ring. Donor **5a** (AET) and **5b** show oxidation potentials similar to those of BEDT-TTF, in spite of the introduction of the electron-withdrawing azulene ring. This result ensures the donor ability of these donors. The substitution of selenium for outer sulfur (**5c**) does not affect the potentials significantly, but replacement of inner sulfur (**5d**) positively shifts both E_1 and E_2 values. The high E_1 and E_2 values for **5e** can be attributed to the electron-withdrawing character of the thiadiazole ring.

The molecular structure of AET was determined by single crystal X-ray analysis (Fig. 3, Tables 2, 3). The C–C bond lengths in the azulene ring are almost equal (about 1.4 Å). This suggests that the aromaticity of the ring is retained even if the

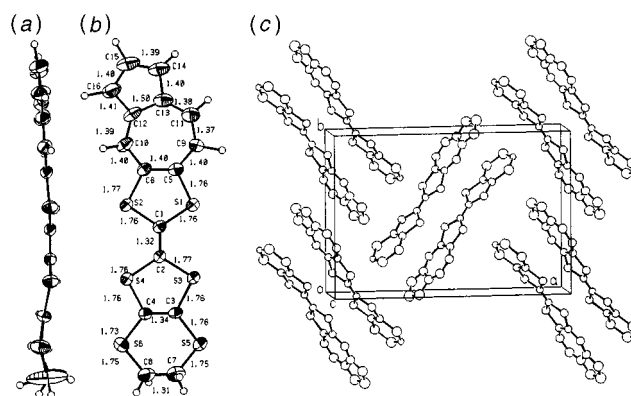
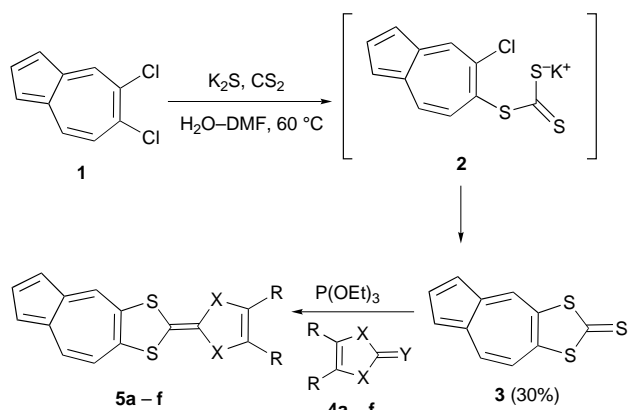


Fig. 3 (a) Side view of the AET; (b) top view of the AET; (c) crystal packing of the AET

Table 2 Crystallographic data for AET and (AET)₂[Pt(dmit)₂]

	AET	(AET) ₂ [Pt(dmit) ₂]
empirical formula	C ₁₆ H ₁₀ S ₆	C ₃₈ H ₂₀ PtS ₂₂
formula mass	394.61	1376.99
colour & shape	dark brown block	brownish black plate
crystal system	monoclinic	monoclinic
space group	<i>P</i> 2 ₁ / <i>n</i>	<i>P</i> 2 ₁ / <i>n</i>
<i>a</i> /Å	19.104(4)	11.619(3)
<i>b</i> /Å	13.057(3)	30.222(4)
<i>c</i> /Å	6.515(2)	6.547(1)
β /°	93.16(2)	97.62(2)
<i>V</i> /Å ³	1622.5(6)	2278.7(7)
<i>Z</i>	4	2
total no. of observed reflections	4224	5218
no. of unique data with $I \geq 3\sigma(I)$	2123	3640
no. of variables	239	288
<i>R</i> ; <i>R</i> _w	0.046; 0.032	0.042; 0.044
maximum peak in final diff. map/Å ³	0.35e	1.49e
minimum peak in final diff. map/Å ³	−0.39e	−1.88e



a X = S, Y = O, R–R = SCH ₂ CH ₂ S	44%
b X = S, Y = O, R–R = SCH ₂ S	49%
c X = S, Y = O, R–R = SeCH ₂ CH ₂ Se	34%
d X = Se, Y = O, R–R = SCH ₂ CH ₂ S	38%
e X = S, Y = S, R–R = =NSN=	5%
f X = S, Y = O, R = I	17%

Scheme 1

Table 3 Selected bond lengths ($d/\text{\AA}$) for $(\text{AET})_2[\text{Pt}(\text{dmit})_2]$

AET		Pt(dmit)	
C(1)–C(2)	1.303(9)	Pt–S(7)	2.270(2)
S(1)–C(1)	1.763(6)	Pt–S(8)	2.273(2)
S(2)–C(1)	1.759(7)	S(7)–C(17)	1.716(6)
S(1)–C(5)	1.742(7)	S(8)–C(18)	1.694(7)
S(2)–C(6)	1.780(7)	C(17)–C(18)	1.366(8)
S(3)–C(2)	1.749(7)	S(9)–C(17)	1.735(6)
S(4)–C(2)	1.759(6)	S(10)–C(18)	1.746(6)
S(3)–C(3)	1.751(7)	S(9)–C(19)	1.737(7)
S(4)–C(4)	1.751(7)	S(10)–C(19)	1.726(7)
C(3)–C(4)	1.339(9)	S(11)–C(19)	1.640(7)

Table 4 Resistivity of cation radical salts

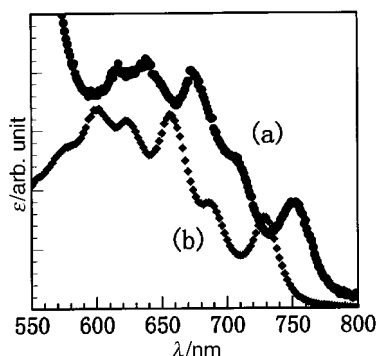
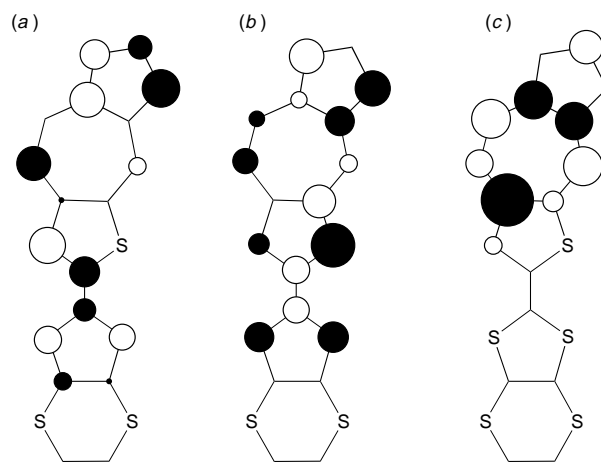
donor (D)	anion (A)	D:A	$\rho_{rt}/\Omega \text{ cm}$	E_a/meV
5a	BF_4^-	—	0.6	45
	ClO_4^-	—	0.3	52
	PF_6^-	2:1 ^a	0.4	50
	AsF_6^-	2:1 ^a	2	62
	$\text{Pt}(\text{dmit})_2^-$	2:1	10 ^b 40 ^c	120 120
5c	PF_6^-	2:1 ^a	3	63
5d	PF_6^-	2:1 ^a	1	23
5f	PF_6^-	3:1 ^a	10	67

^aDetermined by EPMA measurement. ^bMeasured along the a axis.

^cMeasured along the c axis.

ring is attached to the TTF moiety.¹³ This fact is also supported by the absorption in the visible region, which is characteristic of the azulene ring¹⁴ (Fig. 4). The C=C bond lengths as well as the C–S bond lengths in the TTF moiety show normal values compared to those in the known neutral TTF derivatives.¹⁵ The molecular plane bends slightly at S(3) and S(4), which is the same with the molecular structure of the neutral BEDT–TTF.¹⁵ There is a positional disorder in the terminal ethylenedithio fragment as reflected by the elongated thermal ellipsoid for C(7) and C(8) as well as slightly larger atomic displacement parameters ($B_{\text{eq}} = 5.19$ and 4.58 , respectively) of S(5) and S(6). AET molecules are dimerized and the molecules in the dimer are interrelated by the inversion centre as shown in Fig. 3(c). No S...S contact shorter than the sum of the van der Waals radii (3.60 \AA) is observed among the donor molecules.

The molecular orbitals of AET have been calculated by a semiempirical method (MOPAC: PM3 hamiltonian) using the coordinates of neutral AET obtained by X-ray analysis (Fig. 5). The coefficients of the LUMO are distributed on the azulene moiety, and its electronic structure is approximately the same as that of the simple azulene [*cf.* Fig. 2(b)]. On the other hand, the coefficients of the HOMO and the next-HOMO are distributed on both azulene and TTF moieties, presumably because their energy levels are very close to each other.

**Fig. 4** Visible spectrum of (a) AET and (b) 5,6-dichloroazulene**Fig. 5** Schematic representation of the coefficients of the AET for (a) next-HOMO, (b) HOMO and (c) LUMO

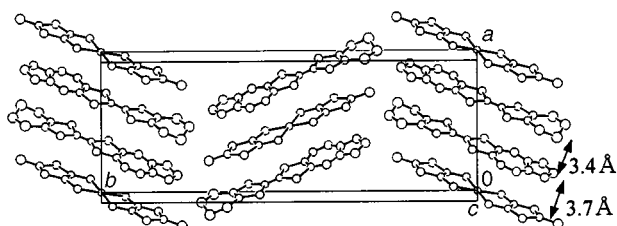
Although this situation would reduce the dipole oscillating effect of the azulene moiety, it is still possible that the excitation of an electron from the HOMO or the next-HOMO to the LUMO causes a change of electric potential at the TTF moiety and thus an attractive interaction between conduction electrons.

Properties of cation radical salts

Cation radical salts of new donors were prepared by galvanostatic oxidation with various kinds of counter anions such as BF_4^- , ClO_4^- , PF_6^- , AsF_6^- and $[\text{Pt}(\text{dmit})_2]^{n-}$. All these salts show rather small resistivities but are semiconductive above room temperature with small activation energies (Table 4).

Since the quality of the crystals is not so good in general, X-ray structural analysis was performed only for $(\text{AET})_2[\text{Pt}(\text{dmit})_2]$. Crystal data are summarized in Table 2. The unit cell contains two mixed columns which are crystallographically equivalent (Fig. 6). In each column, a repeating unit consists of two AET molecules and one $\text{Pt}(\text{dmit})_2$ molecule. The two AET molecules are interrelated by the inversion centre and the $\text{Pt}(\text{dmit})_2$ molecule is located on the inversion centre. The AET molecule is almost planar and there is no positional disorder at the terminal ethylene group. Interplanar distances are 3.4 \AA between AET molecules and 3.7 \AA between AET and $\text{Pt}(\text{dmit})_2$ molecules. Short intermolecular S...S distances are observed only between AET molecules arranged in a side-by-side fashion (Fig. 7).

The bond lengths in the TTF moiety are known to be sensitive to the formal charge, and oxidation of TTF should result in an increase of the central C=C bond length.¹⁶ The central C(1)–C(2) bond length of AET is slightly shorter than that of the neutral AET, and other bond lengths within the TTF moiety are almost the same as those in the neutral one (Table 3). This means that the AET molecule is nearly neutral in this crystal. As for the formal charge of $[\text{Pt}(\text{dmit})_2]^{n-}$, it is difficult to discuss a difference of the formal charge from its Pt–S bond lengths,¹⁷ although a difference of the oxidation state from $n=2$ to $n=0$ is expected to result in a decrease of

**Fig. 6** Crystal packing in $(\text{AET})_2[\text{Pt}(\text{dmit})_2]$

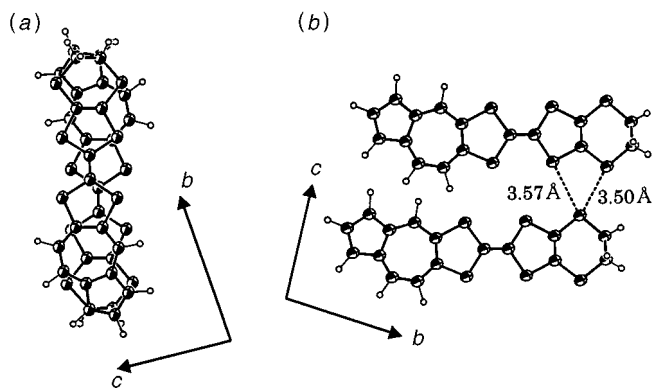


Fig. 7 (a) Overlapping mode of donor molecules; (b) side-by-side contacts between donor molecules in the $(\text{AET})_2[\text{Pt}(\text{dmit})_2]$ crystal

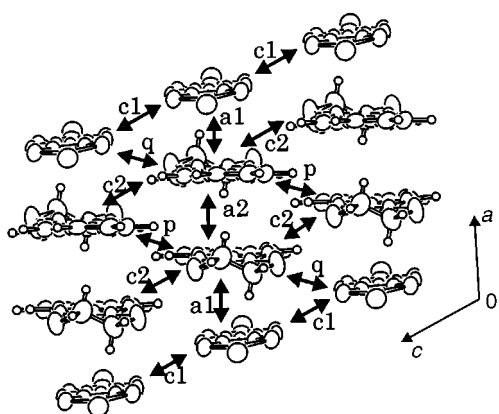


Fig. 8 Molecular arrangement viewed along the b axis

this bond length. The Pt–S bond lengths (about 2.27 Å) are shorter than those in $\text{TTF}[\text{Pt}(\text{dmit})_2]_3$ (about 2.30 Å),¹⁸ which suggests that the $\text{Pt}(\text{dmit})_2$ molecule in our crystal is approximately neutral.

Intermolecular overlap integrals among frontier orbitals [HOMO for AET and LUMO for $\text{Pt}(\text{dmit})_2$] illustrated in Fig. 8 are shown in Table 5. One unknown band parameter is the energy difference (ΔE) between the LUMO and HOMO. Considering that the amount of charge transfer from AET to $\text{Pt}(\text{dmit})_2$ is small and the system is a semiconductor with a band gap (E_g) of 0.24 eV [E_g is twice as large as the activation energy ($E_a=0.12$ eV)], the ΔE value is estimated to be about 0.3 eV so that E_g is consistent with the resistivity measurement. It has been assumed that the transfer integral (t) is proportional to the overlap integral (S), $t = \epsilon S$ ($\epsilon = -10$ eV, ϵ is a constant with the order of the orbital energies of the HOMO and LUMO). The band structure was calculated based on the tight-binding approximation and is displayed in Fig. 9. The highest-lying (mainly) LUMO band is separated far from the (mainly) HOMO bands. Since the degree of the band filling is 2/3, the system is a semiconductor with an energy gap. In this case, the large ΔE value (and thus small charge transfer) is one of the main causes of the semiconductive behaviour. It should

Table 5 Intermolecular overlap integrals (S) of frontier orbitals in $(\text{AET})_2[\text{Pt}(\text{dmit})_2]$

	$S/10^{-3}$
a1	–5.41
a2	–4.54
c1	–0.079
c2	–1.31
p	–0.62
q	–1.02

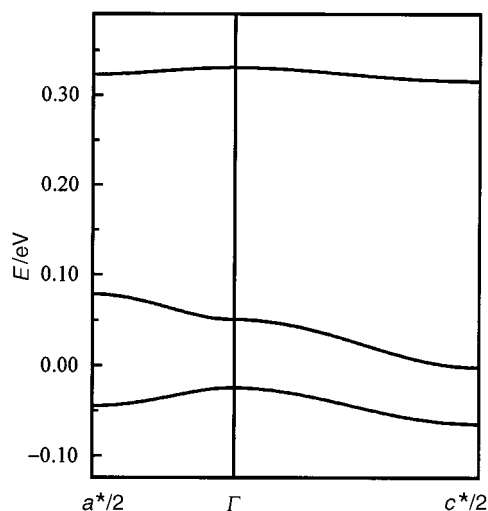


Fig. 9 Band dispersion of $(\text{AET})_2[\text{Pt}(\text{dmit})_2]$ calculated by the tight-binding method. The level of the AET HOMO is the origin of energy.

be noted that the ordinary mixed-stack system is a semiconductor, even if there is enough charge transfer. If the transverse interactions are enhanced, however, the system can achieve a metallic band structure.¹⁹ Indeed, when small ΔE values are adopted, our system exhibits a Fermi surface. Therefore, it would be possible to obtain a metallic system by the choice of an appropriate acceptor.

Conclusion

We have proposed that Little's high-temperature superconductivity theory can be applied to molecular conductors. The azulene moiety of the donor AET retains the electronic structure of the simple azulene, although partial mixing of the azulene HOMO and the TTF HOMO was suggested by semiempirical MO calculations. At present, unfortunately, cation radical salts of the donors are all semiconductive. The crystal and electronic structures of $(\text{AET})_2[\text{Pt}(\text{dmit})_2]$ suggest one condition for the metallic state. Research towards the achievement of the metallic state is in progress.

Experimental

All reactions were carried out under an Ar atmosphere. 5,6-Dichloroazulene²⁰ and units **4a–4f**^{21–24} were synthesized according to the methods described in the literature.

Azuleno [5,6-*d*]-[1,3]-dithiole-2-thione 3

A dimethylformamide (DMF) (300 ml) solution of 5,6-dichloroazulene (10.10 g, 51.3 mmol) was added dropwise into an aqueous solution (30 ml) of potassium sulfide (8.51 g, 77.2 mmol) at room temp. After 15 min, carbon disulfide (50 ml) was also added and the reaction mixture was stirred at 60 °C for 16 h. The resultant mixture was poured into benzene (1 l), and filtered through Celite. This benzene solution was washed with water (500, 300, 300 ml), and dried with MgSO_4 . The solvent was removed under reduced pressure, and the silica gel column chromatography with carbon disulfide as eluent gave pure **3** (3.57 g, 30%) as green fibres. Mp 151–154 °C (decomp.) (Calc. for $\text{C}_{11}\text{H}_6\text{S}_3$: C, 56.37; H, 2.58. Found: C, 56.29; H, 2.77%); (HRMS: Calc. 233.9632. Found 233.9603); δ_{H} ($\text{CDCl}_3\text{-CS}_2$) 7.13 (1H, d, J 10.2), 7.35 (1H, d, J 4.0), 7.42 (1H, d, J 3.7), 7.86 (1H, t, J 3.8), 8.13 (1H, d, J 10.6), 8.20 (1H, s) (J values in Hz throughout).

Synthesis of donors 5a–5f: general procedure

A triethyl phosphite (5 ml) solution of **3** (1 mmol) and unit **4a–4f** was heated to 100 °C for 30 min. It was cooled to room temp., methanol (30 ml) was added and the reaction mixture filtered through a glass filter. The brown solid obtained was purified by silica gel chromatography with carbon disulfide as eluent to afford pure **5a–5f**.

2-(Azuleno[5,6-*d*][1,3]dithiol-2-ylidene)-5,6-dihydro-1,3-dithiolo[4,5-*b*][1,4]dithiine 5a. 44%, mp > 300 °C (Calc. for C₁₆H₁₀S₆: C, 48.69; H, 2.55. Found: C, 48.69; H, 2.73%) (HRMS: Calc. 393.9107. Found 393.9127); δ_{H} (CDCl₃–CS₂) 3.27 (4H, d, *J* 1.3), 6.97 (1H, d, *J* 9.9), 7.14 (1H, d, *J* 4.3), 7.21 (1H), 7.70 (1H, t, *J* 3.8), 7.93 (1H, d, *J* 10.2), 8.04 (1H, s).

2-(Azuleno[5,6-*d*][1,3]dithiol-2-ylidene)-1,3-dithiolo[4,5-*d*]-[1,3]dithiolo 5b. 49%, mp > 300 °C (Calc. for C₁₅H₈S₆: C, 47.33; H, 2.73. Found: C, 47.08; H, 2.28%) (HRMS: Calc. 379.8950. Found 379.8940); δ_{H} (CDCl₃–CS₂) 4.95 (2H, s), 6.97 (1H, d, *J* 10.2), 7.14 (1H, d, *J* 4.3), 7.22 (1H), 7.69 (1H, t, *J* 3.8), 7.94 (1H, d, *J* 10.2), 8.02 (1H, s).

2-(Azuleno[5,6-*d*][1,3]dithiol-2-ylidene)-5,6-dihydro-1,3-dithiolo[4,5-*b*][1,4]diselenine 5c. 34%, mp 286–289 °C (decomp.) (Calc. for C₁₆H₁₀S₄Se₂: C, 39.34; H, 2.06. Found: C, 39.19; H, 2.19%; δ_{H} (CDCl₃–CS₂) 3.35 (4H, s), 6.96 (1H, d, *J* 10.2), 7.11 (1H, d, *J* 4.0), 7.20 (1H, d, *J* 3.6), 7.66 (1H, t, *J* 3.8), 7.92 (1H, d, *J* 9.5), 8.00 (1H, s).

2-(Azuleno[5,6-*d*][1,3]dithiolo-2-ylidene)-5,6-dihydro-1,3-diselenolo[4,5-*b*][1,4]dithiine 5d. 38%, mp 225–228 °C (decomp.) (Calc. for C₁₆H₁₀ S₄Se₂: C, 39.34; H, 2.06. Found: C, 39.18; H, 2.16%; δ_{H} (CDCl₃–CS₂) 3.30 (4H, s), 6.95 (1H, d, *J* 10.3), 7.14 (1H, d, *J* 3.8), 7.23 (1H), 7.69 (1H, t, *J* 4.0), 7.94 (1H, d, *J* 9.6), 8.00 (1H, s).

4-(Azuleno[5,6-*d*][1,3]dithiol-2-ylidene)-[1,3]dithiolo[4,5-*c*][1,2,5]thiadiazole 5e. 5%, mp 268–272 °C (decomp.) (Calc. for C₁₄H₆N₂S₅: C, 46.38; N, 7.73; H, 1.67. Found: C, 46.64; N, 7.45; H, 1.96%) (HRMS: Calc. 361.9135. Found 361.9148); δ_{H} (CDCl₃–CS₂) 7.02 (1H, d, *J* 10.2), 7.19 (1H, d, *J* 3.7), 7.27 (1H, d, *J* 3.3), 7.73 (1H, t, *J* 3.6), 7.99 (1H, d, *J* 10.2), 8.06 (1H, s).

2-(4,5-Diiodo-1,3-dithiol-2-ylidene)azuleno[5,6-*d*][1,3]dithiolo 5f. 17%, mp > 300 °C (Calc. for C₁₄H₆I₂S₄: C, 30.23; H, 1.09. Found: C, 30.15; H, 1.16%; δ_{H} (CDCl₃–CS₂) 6.96 (1H, d, *J* 10.3), 7.13 (1H, d, *J* 3.3), 7.20 (1H), 7.68 (1H, t, *J* 4.0), 7.93 (1H, d, *J* 10.9), 7.99 (1H, s).

Cyclic voltammetry measurements

The cyclic voltammetry experiments were all performed under argon atmosphere at room temp. A solution of tetra(*n*-butyl)ammonium perchlorate–benzonitrile (0.1 M), Pt working and auxiliary electrodes were used. Potentials were referenced *vs.* Ag/0.01 M AgNO₃. Sweep rate was 100 mV s⁻¹ in every experiment.

Preparations of cation radical salts

Cation radical salts of **5a–5f** were obtained by galvanostatic oxidation of a solution containing the donor (*ca.* 8 mg) and the corresponding supporting electrolyte (35–70 mg) as tetra(*n*-butyl)ammonium salts in 1,1,2-trichloroethane (20 ml, containing 5% of ethanol as stabilizing reagent) under an argon atmosphere at 20 °C. An H-shaped cell and platinum wire electrodes (1 mm diameter) were employed and a constant current (0.5 μ A) was applied for 1–4 weeks. Crystals formed in the anode compartment were collected and washed with acetone and *n*-hexane.

Table 6 Semiempirical parameters for Slater-type atomic orbitals

	S		C		H		Pt	
	3s	3p	2s	2p	1s	6s	6p	5d ^a
ζ_1	2.12	1.83	1.63	1.63	1.30	2.55	2.55	6.01(0.633)
ζ_2								2.70(0.551)
$-I_p/\text{eV}$	1.47	0.79	1.57	0.84	1.0	0.67	0.40	0.93

^aTwo Slater exponents were used for the 5d functions. Each is followed in parentheses by the coefficient in the double zeta expansion.

Electrical resistivity measurements

The direct current resistivity measurements were performed with the standard four-probe method. Gold leads (15 μ m diameter) were attached to the crystal with carbon paste.

Crystal structure analysis

X-Ray diffraction data for AET were collected on a MAC Science automatic four-circle diffractometer (MXC18) with graphite-monochromated Mo-K α radiation up to $2\theta = 60^\circ$. The intensities were corrected for Lorenz and polarization effects. The data for (AET)₂[Pt(dmit)₂] were collected on a MAC Science Weissenberg-type imaging plate system (DIP320S). The cell constants were refined by the four-circle diffractometer with monochromated Mo-K α radiation up to $2\theta = 60^\circ$.

The structures were solved by direct methods and refined using full-matrix least-squares analysis using reflections with $I \geq 3\sigma(I)$. An analytical absorption correction was carried out for AET. Anisotropic atomic displacement parameters were used for non-hydrogen atoms. All calculations were performed using TEXSAN the crystallographic software package from Molecular Structure Co.

MO calculations

The molecular orbital calculation was performed using MOPAC93 included in CHEM3D from Cambridge Science Co. The calculation was carried out with the option C.I. = 4.

In order to calculate intermolecular overlap integrals, the HOMO obtained from the extended Hückel MO calculation was used. The calculation was carried out with the use of semiempirical parameters for Slater-type atomic orbitals²⁵ (Table 6).

The authors are grateful to Takeda Chemical Industry Co. Ltd. for the supply of 3,3,4,4-tetrachlorothiophene 1,1-dioxide as a starting material for 5,6-dichloroazulene.

References

- 1 K. Kagoshima, H. Anzai, K. Kajimura and T. Ishiguro, *J. Phys. Soc. Jpn.*, 1975, **39**, 1143; F. Denoyer, F. Comès, A. F. Garito and A. J. Heeger, *Phys. Rev. Lett.*, 1975, **35**, 445.
- 2 J. F. Kwak, J. E. Schirber, R. L. Greene and E. M. Engler, *Phys. Rev. Lett.*, 1981, **46**, 1296.
- 3 J. W. Bray, H. R. Hart, Jr., L. V. Interrante, I. S. Jacobs, J. S. Kasper, G. D. Watkins, S. H. Wei and J. C. Bonner, *Phys. Rev. Lett.*, 1975, **35**, 744.
- 4 D. Jerome, A. Mazaud, M. Ribault and K. Bechgaard, *J. Phys. Lett. (Paris)*, 1980, **41**, 95.
- 5 J. Wosnitzer, *Fermi Surfaces of Low-Dimensional Organic Metals and Superconductors*, Springer Tracts in Modern Physics vol. 134, Springer, Berlin, 1996.
- 6 J. M. Williams, J. R. Ferraro, R. J. Thorn, K. D. Carlson, U. Geiser, H. H. Wang, A. M. Kini and M. H. Whangbo, *Organic Superconductors (Including Fullerenes): Synthesis, Structure, Properties and Theory*, Prentice Hall, Englewood Cliffs, NJ, 1992.
- 7 *Organic Superconductivity*, ed. V. Z. Kresin and W. A. Little, Plenum Press, New York, 1990.
- 8 W. A. Little, *Phys. Rev.*, 1964, **134**, A1416.
- 9 J. Bardeen, L. N. Cooper and J. R. Schrieffer, *Phys. Rev.*, 1957, **108**, 1175.

- 10 D. M. Lemal and G. D. Goldman, *J. Chem. Educ.*, 1988, **65**, 923.
- 11 G. W. Wheland and D. E. Mann, *J. Chem. Phys.*, 1949, **17**, 264; A. G. Anderson and B. M. Steckler, *J. Am. Chem. Soc.*, 1959, **81**, 4941.
- 12 R. M. Hochstrasser and L. J. Noe, *J. Chem. Phys.*, 1969, **50**, 1684.
- 13 J. M. Robertson, H. M. M. Shearer, G. A. Sim and D. G. Watson, *Acta Crystallogr.*, 1962, **15**, 1.
- 14 J. Brunken, *Chem. Ber.*, 1960, **93**, 2572; E. W. Thulstrup, P. L. Case and J. Michl, *Chem. Phys.*, 1974, **6**, 410.
- 15 H. Kobayashi, A. Kobayashi, Y. Sasaki and G. Saito, *Bull. Chem. Soc. Jpn.*, 1986, **59**, 301.
- 16 H. Kobayashi, A. Kobayashi, Y. Sasaki, G. Saito and H. Inokuchi, *Chem. Lett.*, 1984, 183.
- 17 L. Valade, J. P. Legros, M. Bousseau, P. Cassoux, M. Garbaskas and L. V. Interrante, *J. Chem. Soc., Dalton Trans.*, 1985, 783; G. N. Schrauzer, *Acc. Chem. Res.*, 1969, **2**, 72.
- 18 M. Bousseau, L. Valade, J. P. Legros, P. Cassoux, M. Garbaskas and L. V. Interrante, *J. Am. Chem. Soc.*, 1986, **108**, 1908.
- 19 H. Kobayashi, R. Kato, A. Kobayashi and Y. Sasaki, *Chem. Lett.*, 1985, 191.
- 20 S. E. Reiter, L. C. Dunn and K. N. Houk, *J. Am. Chem. Soc.*, 1977, **99**, 4199.
- 21 N. Svensrup and J. Becher, *Synthesis*, 1995, 215.
- 22 R. Kato, H. Kobayashi and A. Kobayashi, *Synth. Met.*, 1991, **41–43**, 2093.
- 23 A. E. Underhill, I. Hawkins, S. Edge, S. B. Wilkes, K. S. Varma, A. Kobayashi and H. Kobayashi, *Synth. Met.*, 1993, **55–57**, 1914.
- 24 T. Imakubo, PhD Thesis, University of Tokyo, 1996.
- 25 R. H. Summerville and R. Hoffmann, *J. Am. Chem. Soc.*, 1976, **98**, 7240.

Paper 7/03737F; Received 29th May, 1997